Design and testing of wind deflectors for roof-mounted solar panels

G. V. Kudav[1], Y. M. Panta[1] & M. Yatsco[2]
[1]*Youngstown State University, Department of Mechanical Engineering, Ohio, USA*
[2]*V&M Star, Youngstown, USA*

Abstract

The amount of solar energy that can be produced in the US and throughout the world has seen an unprecedented potential to fulfill growing energy demand. Solar panels can be installed on the ground or on the roof of a building. Roof mounted solar panels could experience occasional high wind loads especially lift and drag forces. Solar panels are bolted directly onto the roof and are secured using ballasts as counter weights against the wind loads. We propose the use of efficient wind deflectors designed and strategically placed in front of the panels as reported here. The deflectors under study were proven to minimize the wind loads on solar panels, ensuring the safety of civilians and surrounding property.

The present study utilizes wind tunnel testing and computational simulation using the commercial computational fluid dynamics software ANSYS Fluent for a steady, turbulent wind flow (standard k-ε model) over an inclined rooftop-solar panel. The study shows promising results in the prediction of the wind forces for an effectively designed wind management system. As specified earlier, results were compared and validated by both wind tunnel experiments and computational simulations for a meaningful conclusion. Solar panels with various aspect ratios for high incoming wind speeds in the range 40–50 m/s (i.e. 90–110 mph) with several angles of attack were modeled and simulated. We report the analysis of high wind loads on the solar panels leading to the design of an optimized wind deflector to counter such loads. It was concluded that an elliptically profiled wind deflector, with uniformly spaced short fins that were positioned before the tilted panels, was proven to minimize the high wind loads by as much as half, compared to the wind loads without the deflector.
Keywords: rooftop solar panels, solar panel deflectors, wind loads, ballast.

WIT Transactions on Engineering Sciences, Vol 74, © 2012 WIT Press
www.witpress.com, ISSN 1743-3533 (on-line)
doi:10.2495/AFM120021

1 Introduction

Solar power has gained several increasing domestic and commercial applications as a renewable source of energy [1]. The two most common methods of solar panel deployment are on the ground or on the roof. Ground-mounted solar panel racks need open land that can considerably increase initial project investment and also the system installation costs. The more logical and cost saving alternative would be to mount the solar panel racks on the roof of a building without the need to purchase or lease an open lot to install the solar panel system. This also enables the solar panels to be installed even in densely populated locations where space costs are at a premium. Other advantages of installing the racks on the roof are the ease of installation and maintenance in that there is no need to dig holes for the support beams of the solar panel racks as there is for ground-mounted racks.

Earlier research studies indicate that the optimum tilt angles for the solar panels are between 22° and 48° which can allow sufficient sunlight in solar panels. Tilt angles close to about 30° are the best for various regions in the US as indicated by figure 1. One previous study [2] has presented some good strategies for mounting solar panel arrays on roofs. It is important to mention here that these tilt angles are influenced by the latitude of the location and the solar azimuth angle. A recent study [3] reported that wind tunnel experiments can successfully analyze wind uplift on solar panel models. The study also discussed the effect of guide plates for the reduction of lift forces in various experimental configurations of the solar panels. A more recent study revealed the usefulness of wind tunnel experiments and computational fluid dynamics (CFD) analysis for roof-mounted solar photovoltaic arrays in correlating CFD simulation results with the wind tunnel test data [4].

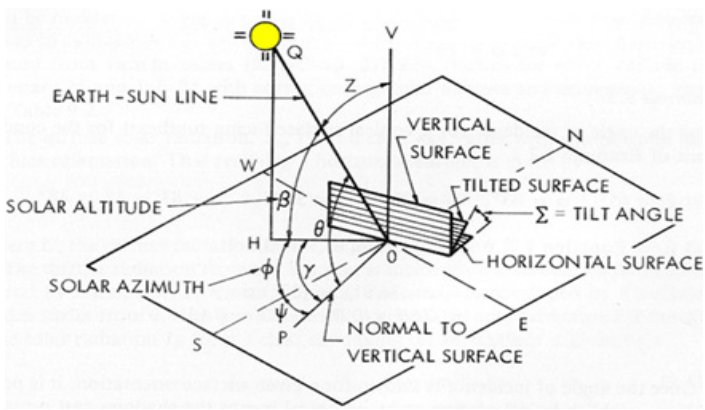

Figure 1: The solar azimuth angle for a photovoltaic array situated in the Northern hemisphere [5].

The solar panel racks can be installed on almost any type of flat roof surface made of tar, gravel, or rubber. Major considerations for the roof-mounted panel racks are wind speed and wind direction resulting in aerodynamics forces or wind loads on the racks. General wind data maps [2] help determine the ranges of wind speeds, their direction, and the angle of attacks in the continental United States throughout the year. Similarly, general wind data maps of other continents and countries can also be used to estimate the ranges of wind speeds and their direction/angle of attacks. Wind loads often necessitate the use of heavy ballast to counter such loads. The ballast weight, however, could exceed the allowable structural load on the roof. Therefore, efficient wind deflecting systems could reduce or ideally eliminate use of ballast.

A recent study revealed the usefulness of wind tunnel experiments and CFD analysis for roof-mounted solar photovoltaic arrays [6]. With the aid of CFD and wind tunnel facilities, the current work presents the design of wind deflectors to minimize the wind loads, especially the drag and lift forces, on the solar panels. The computational analysis comprises the use of CFD software ANSYS Fluent in an iterative mode for one-quarter and full scale models. These results were further validated with wind tunnel tests. Several geometries of wind deflectors were designed and analyzed to minimize wind load reduction and the one that reduced the overall drag and lift forces the most was ultimately chosen and offered to the research sponsor – Northern States Metal, NSM, Youngstown, Ohio, USA [7] – for possible development and marketing.

2 Theory

An algorithm with a set of governing equations including i) the mass/continuity (eqn (1)), ii) the momentum/Navier-Stokes (eqn (2)), iii) the turbulent kinetic energy (eqn (3)), and iv) the dissipation rate equations (eqn (4)) are used for mathematical modeling of the wind flow domain around the solar panel. These governing equations are embedded within ANSYS Fluent to analyze the fluid properties, specifically the lift and drag characteristics on (i) the solar panel and (ii) the solar panel with the deflector placed in front of the panel. Mathematical modeling was carried out in order to analyze the wind forces of the incoming high-speed wind on the given panel model and the deflector. The standard k-ε turbulence model for the turbulent flow was chosen for ANSYS Fluent [8, 9].

Mass – Continuity Equation:

$$\frac{\partial \rho}{\partial t} + \nabla.(\rho \boldsymbol{V}) = \mathbf{0} \tag{1}$$

Momentum – Navier-Stokes Equations:

$$\rho\left[\frac{\partial \boldsymbol{V}}{\partial t} + \boldsymbol{V}\cdot(\nabla \boldsymbol{V})\right] = -\nabla p + \mu \nabla.(\nabla \boldsymbol{V}) + \boldsymbol{f} \tag{2}$$

$$\frac{\partial}{\partial t}(\rho k) + \frac{\partial}{\partial x_i}(\rho k u_i) = \frac{\partial}{\partial x_j}\left[\left(\mu + \frac{\mu_t}{\sigma_k}\right)\frac{\partial k}{\partial x_j}\right] + P_k + P_b - \rho\epsilon - Y_M + S_k \quad (3)$$

$$\frac{\partial}{\partial t}(\rho \epsilon) + \frac{\partial}{\partial x_i}(\rho \epsilon u_i) = \frac{\partial}{\partial x_j}\left[\left(\mu + \frac{\mu_t}{\sigma_\epsilon}\right)\frac{\partial \epsilon}{\partial x_j}\right] + C_{1\epsilon}\frac{\epsilon}{k}(P_k + C_{3\epsilon}P_b) - C_{2\epsilon}\rho\frac{\epsilon^2}{k} + S_\epsilon \quad (4)$$

$$\mu_t = \rho C_\mu \frac{k^2}{\epsilon} \quad (5)$$

where the nomenclature for the symbols has the usual meaning and they are defined below [7]:

$\boldsymbol{V}$ = total velocity vector of the fluid
$u, v, w \equiv$ x-, y-, and z-components of the velocity, respectively
$\boldsymbol{f}$ = body forces
k = turbulent kinetic energy
ε = the rate of dissipation.
$\boldsymbol{\mu_t}$ = the turbulent viscosity
$G_k \equiv$ generation of turbulent kinetic energy due to the mean velocity gradient
$G_b \equiv$ generation of turbulent kinetic energy due to buoyancy
$Y_M \equiv$ contribution of the fluctuating dilatation in compressible turbulence overall dissipation rate
$S_k \equiv$ user defined source term
$S_\varepsilon \equiv$ user defined source term

Other arbitrary constants in Eqns. (3) and (4) are used from the ANSYS Fluent Manual: $C_{1\varepsilon} = 1.44$, $C_{2\varepsilon} = 1.92$, $C_\mu = 0.09$, $\sigma_k = 1.00$, and $\sigma_\varepsilon = 1.3$. These values are acceptable for wall-bounded and free shear flows and are appropriate for a CFD study of solar panel racks positioned in a wall-bounded fluid domain [8, 9].

3 Methodology

As ballast for the solar panel to add substantial weight on a roof mounting, a wind deflector was conceptualized as an alternative solution to reduce or replace the use of such ballast. Based on the study, it was recommended that wind deflectors were placed on all sides of the solar panel racks as a complete wind management system to reduce the head-wind and side-wind effects. If all sided wind deflectors are not economically viable, the wind deflector on the front is highly recommended to minimize the head-wind effects. Although the wind deflector itself will add a minimal weight on the roof it is negligible compared to that of ballast. Multiple deflectors of various surface profiles were designed that

included vertical, inclined, parabolic, elliptic and elliptic with fins shapes. Only a sketch of the elliptic deflectors is shown in figure 2.

Wind flows over the physical model with and without a deflector were tested for wind forces using wind tunnel instruments. Similarly, wind flows with and without a deflector were simulated, and analyzed for wind forces using ANSYS Fluent software. Based on the preliminary CFD analysis among the deflector shapes for high winds, an elliptic finned-deflector (figure 2(b)) was chosen for further analysis by CFD simulation and testing in the wind tunnel for its relative superior performance.

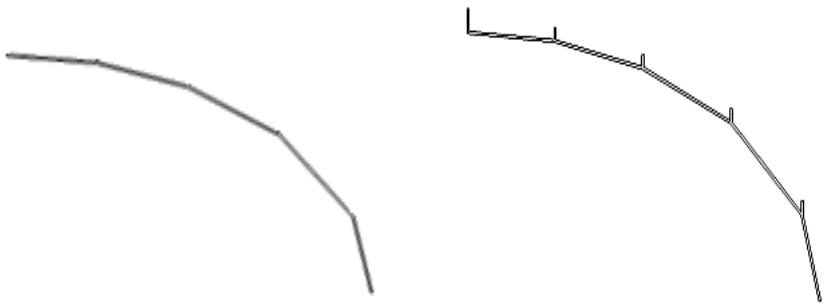

(a) (b)

Figure 2: Side views of the deflector: (a) elliptic, (b) elliptic plus fins.

As mentioned, two methods that included computations using CFD simulations and experiments using wind tunnel testing were employed for wind load analysis. These methodologies are given below.

3.1 Methodology I: computations/simulations

Computational analysis involves solving a problem through the use of an algorithm and mathematical model. ANSYS Fluent software that combines numerical techniques with the intricacies of fluid flow is employed for the modeling of wind flow over the solar panel. The software was built to model and analyze many types of laminar and turbulent fluid flows. The software has different packages and add-ons that allow one to model various geometries with the chosen flow models. The software comes with geometry modeling software, called ANSYS Design Modeler. The remaining add-ons include ANSYS Meshing, ANSYS Fluent, and CFD Post. Details of the ANSYS Fluent, computational models/simulations for the wind flow analysis of the rooftop solar panel racks are discussed in the sections that follow.

3.1.1 CFD software

The procedure to set-up and run a successful simulation in ANSYS Fluent, for a fluid flow problem, consists of a series of steps that are completed sequentially. The procedure is outlined as preprocessing, processing, and post-processing. The

algorithm, descretization technique and the convergence criteria of ANSYS Fluent are summarized below:
1. Construction of the geometrical models using ANSYS Design Modeler.
2. Division of the fluid domain into discrete volumes using ANSYS Meshing.
3. Modeling using ANSYS Fluent (figure 3).
4. Defining the boundary conditions and fluid properties.
5. Solving in Fluent until a converged solution is achieved (eqn. (6)).

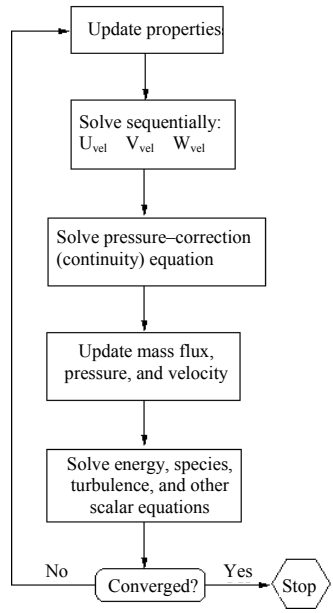

Figure 3: Pressure-based segreagated algorithm used in ANSYS Fluent [9].

3.1.1.1 Pressure-based segregated algorithm The pressure-based solver uses an algorithm to solve for the governing equations in a sequential order with an iterative process as shown in figure 3.

3.1.1.2 Discretization technique ANSYS Fluent utilizes a discretization technique to turn a general scalar equation into an algebraic equation which enables the equations to be solved numerically. The governing equations are integrated about each of the volumes created during the meshing process.

$$\sum_{f}^{Nfaces} \rho_f \vec{v}_f \phi_f \cdot \vec{A}_f = \sum_{f}^{Nfaces} \Gamma_\phi \nabla \phi_f \cdot \vec{A}_f + S_\phi V \tag{6}$$

where

$N_{faces} \equiv$ number of faces enclosing the cell

$\phi_f \equiv$ value of ϕ convected through the face f

$\rho_f \vec{v}_f \cdot \vec{A}_f \equiv$ mass flux through the face f

$\vec{A}_f \equiv$ area of face f

$\nabla \phi_f \equiv$ gradient of ϕ at face f

$V \equiv$ cell volume

3.1.1.3 Convergence criteria The use of a numerical modeling technique requires ways to measure the validity and accuracy of the simulated solution. The convergence criteria in ANSYS Fluent depend on the type of model chosen. These residuals, depending on the type of model selected, involve x- and y-components of the velocities, k and ε that include continuity, momentum, turbulence, and energy.

3.1.2 Computer models and simulations

When modeling the fluid domain surrounding a solar panel using the CFD software, incompressible, steady, Newtonian fluid was assumed of a turbulent nature with no buoyancy effects and no heat considerations. The layout of the flow fields for two computer models that include five solar panels and five solar panels with a deflector at the front are shown in figures 4(a) and 4(b). The reduction in the wind loads on the panel using the wind deflector as predicted by CFD results are discussed in a subsequent section below.

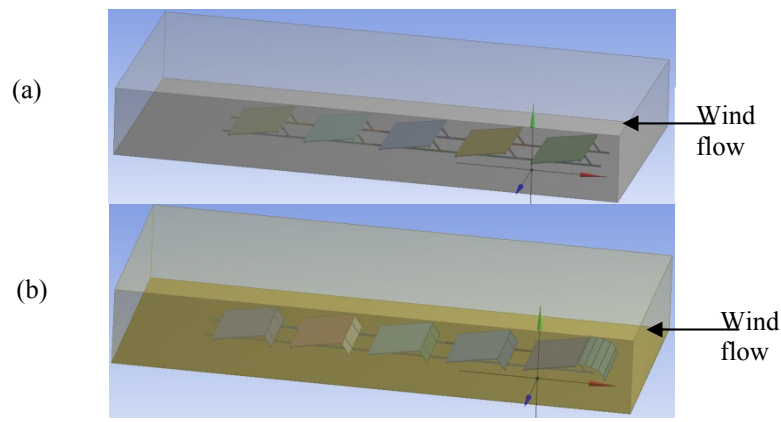

Figure 4: Layout of the flow field for CFD simulation: (a) five solar panels, and (b) five solar panels with a deflector at the front [8].

3.2 Methodology II: experimentations

It is a well-known fact that CFD analysis alone is not an absolute measure of the accuracy in the design of any turbulent flow management system due to inherent uncertainty in the turbulence parameters in the flow field. However, comparisons between results from wind tunnel tests and CFD simulations for a few benchmark models provide the degree of confidence required in the implementation of the design at reduced cost and time. As full scale models were too large to fit into our wind tunnel test section, quarter-scale models were developed and tested in our university's wind tunnel facility. All full-scale solar panel racks that were investigated in this study were at an inclination of 10^o with respect to the horizontal axis for a wind speed of 49 m/s (110 mph).

3.2.1 Wind tunnel instrumentation

The experimental analysis consisted of conducting multiple wind tunnel tests of quarter-scale rooftop solar panel racks and wind deflectors. Figure 5 shows the schematic of the test setup. The fan motor speed was controlled using VFD (PowerFlex-4M, Allen-Bradley) to generate variable input frequencies to the motor that translates into variable wind speeds in the tunnel as inlet wind speed The VFD was actuated via a laptop (Dell E5500) utilizing LABVIEW v8.6 drivers and National Instruments' module NI 9264 by providing voltage in the range of 0~10 Vdc. At each motor rpm, the pitot- static tube that was connected to an electronic pressure sensor (Model 20 INCH D-MV R8B22-58 supplied by All Sensors) measured the pressure difference ($P_0 - P_\infty$), where P_0 is the stagnation pressure and P_∞ is the static pressure in the wind tunnel. The pressure sensor outputs a dc voltage to NI 9219 with a supplied excitation voltage of 2.5 Vdc. Then through a calibration procedure provided by All Sensors, the voltage was converted to a pressure difference in inches of water.

Through Bernoulli's equation, the pressure difference was converted to wind speed in mph. The NI modules interfaced with the NI DAQ module cDAQ-9172 and were controlled by the LABVIEW program. The wind tunnel was calibrated by recording wind speeds at various input frequencies from 0 to 80 Hz in order to interpolate between the wind speed and the corresponding input frequency. The models to be tested were to be mounted on a melamine board. Four load cells (FUTEK's model LCF300:50-lb) were used to record either lift or drag forces. The load cells operate on a full Wheatstone bridge. NI 9237 provided the bridge circuitry. Through a calibration equation provided by FUTEK, the output dc voltage was converted to a force in lbf and then to N through LABVIEW.

3.2.2 Physical models and testing

The load cells were installed with two orientations in order to measure the two major wind forces; namely lift (vertical) and drag (horizontal) forces, for several incoming wind speeds. Following figure 5, figures 6 to 8 below show the wind tunnel and solar panel/load cell setup for wind lift and drag force measurements. The results that were obtained from the wind tunnel analysis were then used to verify the CFD simulations.

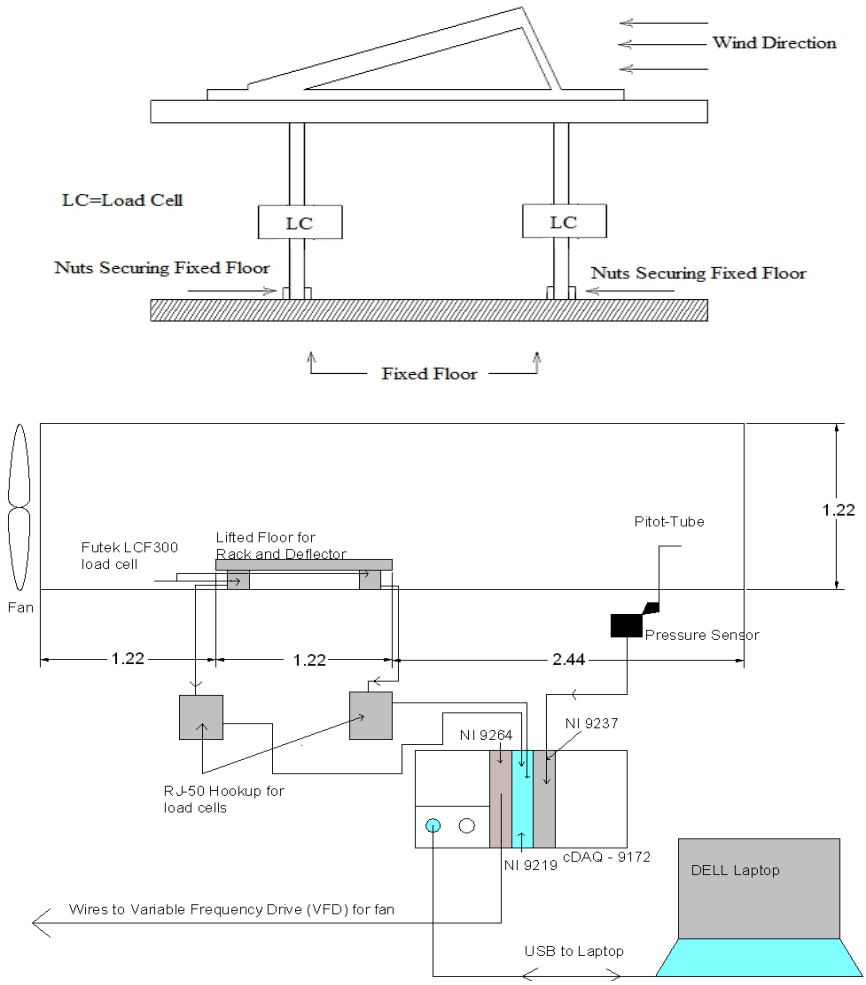

Figure 5: Wind tunnel test setup (all dimensions are in m).

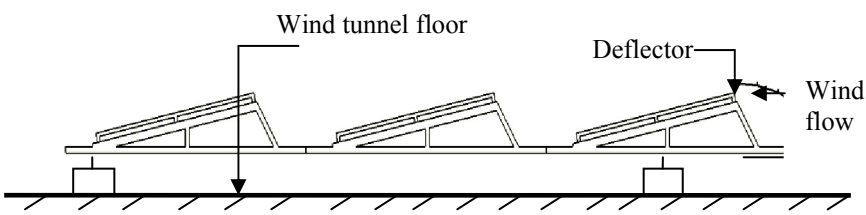

Figure 6: Deflector-panel orientation for a 3-rack system in the wind tunnel.

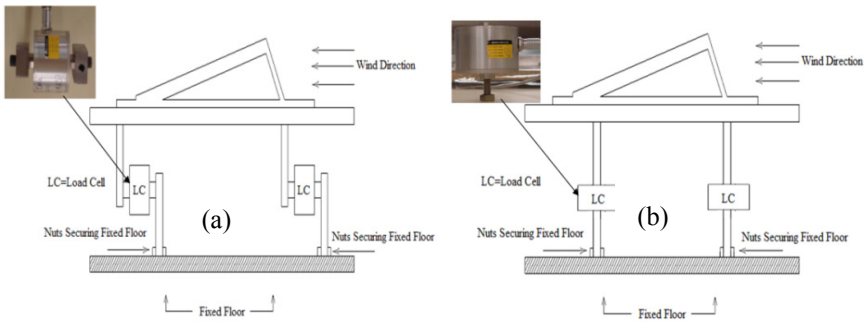

Figure 7: Load cell placement: (a) horizontal for the lift; (b) vertical for the drag force measurement.

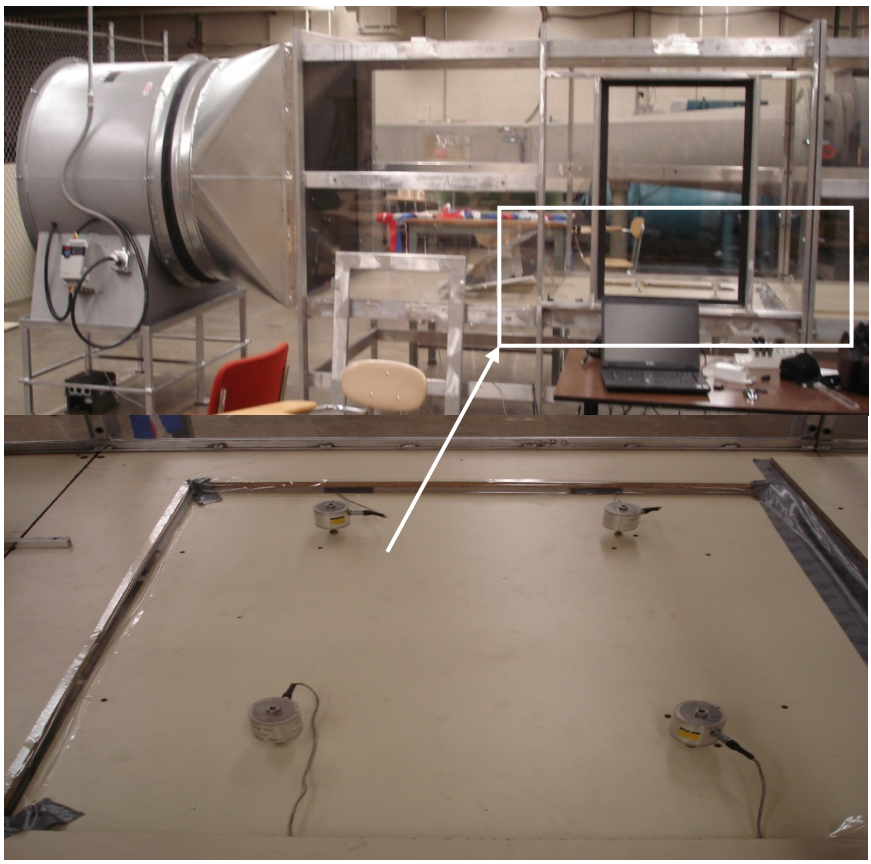

Figure 8: Wind tunnel instrumentation showing load cells on the testing floor (zoomed and shown) for wind uplift force measurement.

4 Results and discussions

The results we report here are presented in the two subsections below. First the wind loads measured for scaled models in the wind tunnel and predicted by CFD analysis are presented followed by the CFD results for the full scale model only.

4.1 Wind tunnel results

Measurements were recorded at four different speeds: 6.7, 9.0, 11.2, and 12.0 m/s (15, 20, 25, and 27 mph). For all the test configurations of the scaled models, the lift and drag forces increased as the wind speed increased from 6.7 m/s (15 mph) to 12 m/s (27 mph) as expected due to the forces being proportional to the square of wind speed. For rack-only arrangement, the minimum and maximum lift forces were 5.34 N and 16.90 N respectively while for the rack-with-deflector system the minimum and maximum lift forces were 2.67 N and 7.56 N respectively. Therefore, it can be concluded solely from the wind tunnel test data that using the deflector reduces the lift forces for the rack-deflector arrangement by approximately 50% for the speeds tested while the drag forces have minimal changes.

4.2 CFD simulation results compared with the wind tunnel test data

As shown in table 1, the use of the deflector reduced wind uplift by 51.29%, but increased the drag force by 28.33%. It should be noted that positive values for the forces represent a reduction and vice versa. The CFD analysis estimated a net reduction of 37.14% and 9.16% for the lift and drag forces, respectively. A similar trend was found in the experimental and computational analysis of the three-rack model with and without deflector.

Table 1: Wind tunnel test data and CFD results for quarter-scale models with input wind velocity=12 m/s – comparison in %.

Quarter-Scale Models for wind speed =12 m/s	Wind Tunnel Vs CFD Difference in %	With Deflector, Reduction in Wind Loads as Measured by			
		Wind Tunnel Tests, %		CFD Simulations, %	
	Lift., FL	Lift., FL	Drag, FD	Lift., FL	Drag, FD
Single Rack Only	27.84	51.29	-28.33	37.14	9.16
Single Rack and Deflector	6.88				
3 Racks Array	28.27	45.61	-26.25	54.09	20.54
3 Racks Array and	8.27				

For a single-rack model, the percentage reduction was 54.29% and 37.14% for experimental and computational results, respectively. The percentage reduction was even closer when the two methods were compared for the three-rack model with deflector: 45.61% for experimental uplift and 54.09% for computational uplift. In terms of drag results, the experimental results resulted in slight additions to the drag force, for both single-rack and three-rack models using the deflector, the addition was around 25%. This addition in wind drag is expected as the addition of the deflector with the rack arrays will somewhat

increase the amount of drag force. When the respective drag and uplift forces are compared for both the scenarios of single-rack only and three-rack array, drag forces were ~70% smaller than the wind uplifts. This comparison explains that the reduction in wind uplifts is more crucial than the wind drag forces for design and installation purposes.

5 Conclusion

We conclude that an elliptic deflector with equally spaced short fins when placed in front of the panel rack greatly reduces uplift on the panels. Wind tunnel experiments showed a slight increase in drag force when a deflector was placed at the front. This is due to the fact that the deflector acts as a bluff body obstruction to the wind flow over the panel. There is a close agreement between computational results and the wind tunnel test data in terms of the calculation of lift forces; however, drag forces were not compared. Lift forces were mainly responsible for the structural stability of solar panels under high winds. It was also noted that a selective grid scheme and refinement in the flow domain have a significant influence and improve CFD results, but lead to much longer simulation run times and convergence. It was concluded that an elliptically profiled wind deflector with uniformly spaced short fins, positioned before the tilted panels, minimizes the high wind loads by as much as 50% compared to the wind loads without its use. Details of the study are currently being reviewed and will also be published in a journal paper.

Acknowledgement

This work was funded in part by Northern States Metal, Inc., Austintown, Ohio, USA.

References

[1] Spratley, W.A., 1998, Solar Rooftops as Distributed Resources, *The Electricity Journal* 11, pp. 40.
[2] Addressing http://www.nafcointernational.com on 02/01/2012 *NAFCO International Inc, 2006-2011, Fond Du Lac, WI, USA.*
[3] Barkaszi, S.F. and Dunlop, J.P., 2001, Discussion of Strategies for Mounting Photovoltaic Arrays on Rooftops, *Proceedings of Solar Forum 2001, Solar Energy: The Power to Choose*, April 21-26, Washington D.C., pp. 6.
[4] Chung, K., Chang, K., Liu Y., 2008, Reduction of wind uplift of a solar collector model *Journal of Wind Engineering and Industrial Aerodynamics*, 96, pp. 1294.
[5] Yatsco, M. 2011, Numerical Analysis and Wind Tunnel Validation of Wind Deflectors for Rooftop Solar Panel Racks. *Master's Thesis, School of Graduate Studies & Research, Youngstown State University, Youngstown, Ohio, USA.*

[6] Meroney, R.N., Neff, D.E., 2010, *Wind effects on roof-mounted solar photovoltaic arrays: CFD and wind-tunnel evaluation,* The Fifth Computational Wind Engineering (CWE2010), Chapel Hill, North Carolina, May 23-27.
[7] Addressing http://www.extrusions.com/ on 02/01/2012 *Northern States Metals, Inc., Youngstown, OH, USA.*
[8] Jiyuan Tu, Guan Heng Yeoh, and Chaoqun Liu, 2008, *Computational Fluid Dynamics: A Practical Approach*, Butterworth-Heinemann.
[9] Addressing http://www.ansys.com/ on 02/01/2012 *ANSYS Customer Portal for Fluent Documentation and User Manuals.*